ORAL/POSTER REFERENCE: to be assigned

Anti-plane shear crack growth in piezoceramics: change of electric field and displacement direction

G.C. Sih[1,2,3], B. Liu[2], Z.F. Song[3], W.F. Ren[2,3]

[1] Institute of Mechanics, Chinese Academy of Sciences, Beijing 100080, China
[2] Institute of Engineering Mechanics, Hebei University of Technology, Tianjin, 300130, China
[3] School of Advanced Science and Technology, Xi'an Jiaotong University, Xi'an, 710049, China

ABSTRACT

Volume energy density factor is derived to evaluate the crack growth behavior under the electric field/shear stress boundary conditions for the PZT-4 and PZT-5H piezoelectric ceramics. Positive electric field is found to enhance anti-plane shear crack growth while negative electric field tends to retard crack growth. This result is similar to that obtained for in-plane crack extension. Crack growth solutions for electric displacement/shear strain boundary conditions, however, suggest that positive electric displacement would retard anti-plane shear crack growth while the opposite would occur for negative electric displacement. It is anticipated the same conclusion would hold for in-plane crack extension, a result that deserves future investigation.

KEYWORDS

Anti-plane shear, Crack growth, Electric displacement, Piezoelectric ceramics, Shear stress

1. INTRODUCTION

Anti-plane shear crack models have been used primarily as a guide for analyzing in-plane crack problems because they are simple to solve and behave similar to plane crack extension. Cracking of piezoelectric materials such as barium titanate and lead zirconate titanate ceramics has added complexities because of the electro-mechanical coupling effects. They possess the special features that when deform an electric field is produced and when subjected to an electric field deformation is pronounced. Such properties are induced through a process referred to as poling such that the materials become transversely anisotropic. In this spirit, the anti-plane shear crack model will be adopted in this work to better understand the in-plane crack growth enhancement and retardation behavior.

One of the unexplained cracking phenomena in piezoelectric ceramics is concerned with the situation that a crack tends to extend longer when the electric field is directed in the pole direction. If the electric field opposes the pole direction, the crack extends shorter. Past attempts [1-4] have provided many reasons why the theoretical and experimental results did not agree but failed to emphasize why they should. Only recently, the volume energy density criterion [5,6] gave results that are physically sound and did not contradict with observed data. The energy release rate remain unchanged if the electric field direction is reversed with reference to that of the pole.

The vulnerable situation for a piezoceramic with a pre-existing crack under anti-plane is for the crack edge to be parallel with the axis of longitudinal shear and transverse anisotropic which coincides with the poling direction. In contrast to in-plane extension the applied electric field would be normal (anti-plane shear) to the pole direction rather than being parallel to each other (in-plane extension). Hence, positive and negative electric field should be referred to the coordinate axes rather than the poling direction. The difference between a positively and negatively applied electric field in anti-plane shear is to reverse the direction of poling. What is physically meaningful is to identify the combination of boundary conditions, applied field direction and material symmetry that would enhance or retard crack growth. Moreover, inappropriate use of fracture criterion could lead to results that would violate the first principle. The energy release rate criterion shows that a positive crack driving force could become negative by increasing the absolute value of the applied electric field [7,8].

2. ANTI-PLANE SHEAR CRACK

Consider the anti-plane shear of a line crack of length 2a in a transversely isotropic piezoelastic material. Referring to Fig. 1(a), the crack lies in the xy-plane while the poling direction coincides with the z-axis. At infinity, either the pair (τ_∞; E_∞) or (γ_∞; D_∞) are specified. The uniform shear stress and strain are τ_∞ and γ_∞, respectively whereas E_∞ and D_∞ are the uniform electric field and displacement, respectively.

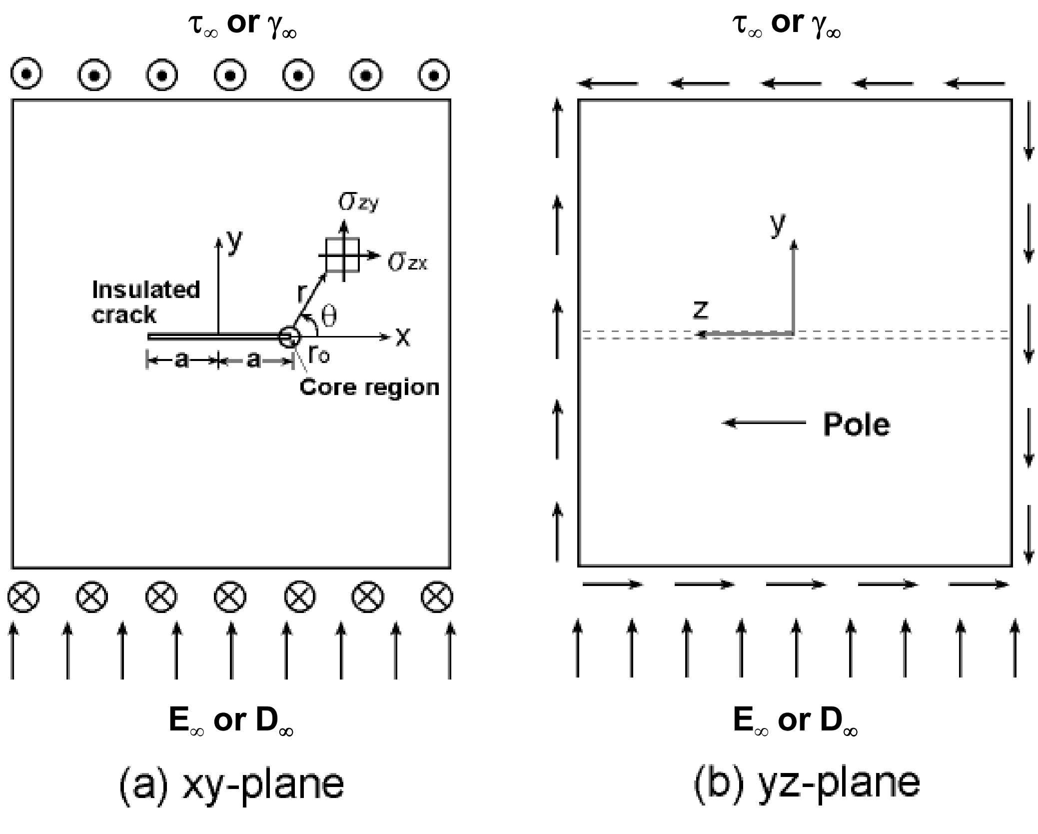

Fig. 1 Schematics of anti-plane shear crack and near tip element

2.1 Basic equations

Under anti-plane shear, there prevails only two pairs of stress and strain (σ_{zx}; γ_{zx}) and (σ_{zy}; γ_{zy}) which are functions of x and y. The in-plane electric and displacement field possess the components (E_x; E_y) (D_x; D_y), respectively. In the absence of body forces and charges, the equations of equilibrium are given by

$$\frac{\partial \sigma_{zx}}{\partial x} + \frac{\partial \sigma_{zx}}{\partial y} = 0, \qquad \frac{\partial D_x}{\partial x} + \frac{\partial D_y}{\partial y} = 0. \tag{1}$$

On the crack surface, the tractions T_z and/or surface charges q can be specified:

$$T_z = \sigma_{xy} n_x + \sigma_{yx} n_y, \qquad -q = D_x n_x + D_y n_y \tag{2}$$

where n_x and n_y are components of the unit normal vector. The constitutive relations take the forms

$$\sigma_{zx} = c_{44}\gamma_{zx} - e_{15}E_x, \qquad \sigma_{zy} = c_{44}\gamma_{zy} - e_{15}E_y \tag{3}$$

and

$$D_x = e_{15}\gamma_{xz} + \in_{11} E_x, \qquad D_y = e_{15}\gamma_{yz} + \in_{15} E_y. \tag{4}$$

only three material constants need to be specified; they are c_{44} (elastic), e_{15} (piezoelectric) and $\in_{11}$ (dielectric),

2.2 Conditions far away and on crack

Referring to Fig. 1(a), a uniform shear stress field τ_∞ or strain field γ_∞ together with uniform electric field E_∞ or electric displacement D_∞ can be specified, i.e.,

$$\sigma_{zy} = \tau_\infty \quad \text{or} \quad \gamma_{zy} = \gamma_\infty \quad \text{for } x^2 + y^2 \to \infty, \tag{5}$$

and

$$E_y = E_\infty \quad \text{or} \quad D_y = D_\infty \quad \text{for } x^2 + y^2 \to \infty. \tag{6}$$

Note that poling is in the positive z-direction.

The conditions on the crack surfaces are to be free of surface tractions and surface charges. They are written as

$$\sigma_{zy} = 0, \quad D_y = 0 \quad \text{for } |x| < a; \quad |y| = 0. \tag{7}$$

The solution for this problem is well known [7,8]. The r and θ functions for those quantities referred to the x- and y- direction can be written as

$$\text{x-component: } -\frac{1}{\sqrt{r}}\sin\frac{\theta}{2} + \cdots, \qquad \text{x-component: } \frac{1}{\sqrt{r}}\cos\frac{\theta}{2} + \cdots. \tag{8}$$

Refer to Fig. 1(b) for the polar coordinates measured from the crack tip. The $1/\sqrt{r}$ singularity is the same as that found for the corresponding anti-plane shear crack in elasticity.

3. Volume energy density function and factor

The volume energy density in an element ahead of the crack, Fig. 1(b), can be computed from

$$\frac{dW}{dV} = \frac{1}{2}(\sigma_{xz}\gamma_{xz} + \sigma_{yz}\gamma_{yz}) + \frac{1}{2}(D_x E_x + D_y E_y). \tag{9}$$

Eq. (8) indicate that the singular term would dominate as $r \to 0$, the crack tip. It follows that dW/dV in eq. (9) would depend on 1/r and can be expressed as

$$\frac{dW}{dV} = \frac{S}{r}, \tag{10}$$

where r is the distance from the crack tip such that $r \geq r_o$. The core region with radius r_o is excluded from the analysis.

For the loading in Fig. 1(a), the crack would extend along the x-axis θ = 0 where dW/dV reaches a critical value $(dW/dV)_c$ that is characteristic of the PZT material. In view of eqs. (8), all quantities referred to the x-direction would vanish and those referred to the y-direction for $\theta = 0$ can be expressed as

$$\sigma_{zx} = -\frac{K_{III}^{\tau}}{\sqrt{2\pi r}}, \qquad \gamma_{zy} = \frac{K_{III}^{\gamma}}{\sqrt{2\pi r}}, \qquad E_y = \frac{K_E}{\sqrt{2\pi r}}, \qquad D_y = \frac{K_D}{\sqrt{2\pi r}} \tag{11}$$

which can be substituted into eqs. (9). Comparing the result with eq. (10) gives the energy density factor

$$S = \frac{1}{4\pi}(K_{III}^{\tau} K_{III}^{\gamma} + K_E K_D)\,. \tag{12}$$

For an element situated at $r = r_o$ and $\theta = 0$, the condition of $(dW/dV)_c$ is equivalent to $S = S_c$. The intensity factors in eqs. (12) stand for

$$\begin{aligned} K_{III}^{\tau} &= (c_{44}F_j - e_{15}G_j)\sqrt{\pi a}\,, \qquad & K_{III}^{\gamma} &= F_j\sqrt{\pi a} \\ K_D &= (e_{15}F_j + \in_{11} G_j)\sqrt{\pi a}\,, \qquad & K_E &= G_j\sqrt{\pi a} \end{aligned} \tag{13}$$

where j = I and II correspond to the two different types of boundary conditions (τ_∞; E_∞) and (γ_∞; D_∞) to be considered. They shall be referred to as Case I and II.

Case I specifies τ_∞ and E_∞. The contractions F_I and G_I in eqs. (13) given by [7]:

$$F_I = \frac{\tau_\infty + e_{15}E_\infty}{c_{44}}, \qquad G_I = E_\infty \tag{14}$$

Putting eqs. (14) into (13) and normalizing eq. (12) with respect to $\tau_\infty^2 a/(4c_{44})$, it can be shown that

$$S/(\frac{\tau_\infty^2 a}{4c_{44}}) = 1 + 2e_{15}p + (c_{44} \in_{11} + e_{15}^2)p^2, \quad \text{Case I} \tag{15}$$

where $p = E_\infty/\tau_\infty$ is a load factor.

Case II specifies γ_∞ and D_∞. The quantities F_j and G_j in eqs. (13) for j = II are known from [7]. They can be put into eq. (12) to render

$$S/(\frac{\gamma_\infty^2 a}{4 \in_{11}}) = (c_{44} \in_{11} + e_{15}^2) - 2e_{15}q + q^2, \quad \text{Case II} \tag{16}$$

where $q = D_\infty/\gamma_\infty$ is a load factor.

Eqs. (14) and (15) show that the volume energy density factor S could increase or decrease with reference to the ratios of the electric field to shear stress or electric displacement to shear strain depending on the properties of piezoelectric materials.

4. Crack growth criterion

The form of eq. (10) has been used as a criterion [9,10] for crack initiation and growth. A crack is assumed to grow in segments of $r_1, r_2, \ldots, r_j, \ldots, r_c$ after dW/dV in an element at $r = r_o$ shown in Fig. 1(b) has reached $(dW/dV)_c$, i.e.,

$$\left(\frac{dW}{dV}\right)_c = \frac{S_1}{r_1} = \frac{S_2}{r_2} = \cdots = \frac{S_j}{r_j} = \cdots = \frac{S_c}{r_c} = \text{const.} \tag{17}$$

The first increment r_1 is measured from the core region r_o. Hence, the half crack length would increase from a to a+ r_o+ r_1. Each subsequent step can be treated in the same way.

4.1 Effect of electric field and displacement reversal

The effect of electric field and displacement will be examined. Now, let the superscripts +, 0, - be attached to those quantities that refer, respectively, to E_∞ or D_∞ that are positive, zero, and negative. Positive E_∞ or D_∞ corresponds to the positive direction of the coordinate axis. The corresponding crack growth segments are r_j^+, r_j^o and r_j^- while the volume energy density factors are S_j^+, S_j^o and S_j^- where j = 1, 2, etc. It follows from eq. (17) that for the jth segment of crack growth yield the expression.

$$\frac{S_j^+}{r_j^+} = \frac{S_j^o}{r_j^o} = \frac{S_j^-}{r_j^-}, \qquad j = 1, 2, \text{etc.} \tag{18}$$

Once the energy density factors are known, the crack growth segments can be computed for different boundary conditions to examine how the direction of applied electric field displacement would affect crack growth. Numerical results will be made available for the PZT-4 and PZT-5H piezoelectric materials. Their elastic, piezoelectric and dielectric constants can be found in Table 1.

TABLE 1

Elastic piezoelectric and dielectric constants

Material	Material constants		
	$c_{44} \times 10^{10}$ (N/m^2)	e_{15} (C/m^2)	$\in_{11} \times 10^{-10}$ (C/Vm)
PZT-4	2.56	13.44	60
PZT-5H	3.53	17.00	151

4.2 Case I: Positive and negative electric field

Note from eq. (15) that a change in the sign of p, i.e., positive and negative E_∞ would affect the value of the energy density factor S. Using the case of E_∞= 0 or $S/(\tau_\infty^2 a/4c_{44}) = 1$ as reference, the ratio S_1^+/S_1^o and S_1^-/S_1^o can be calculated. This also gives r_1^+/r_1^o and r_1^-/r_1^o because they are directly proportional, eq. (18). The numerical results are summarized in Table 2 for different values of p = E_∞/τ_∞. Plotted in Fig. 2 are the numerical values in Table 2. Both curves go through the coordinate p = 0 and $r_1^\pm/r_1^o$ =1. The crack growth segment is greater than r_1^o for positive E_∞ and smaller than r_1^o for negative E_∞. This indicates that +E_∞ and -E_∞ would enhance and retard crack growth. Such a trend continues to prevail for the subsequent crack growth segments because of the relation [11]

TABLE 2

. Normalized first crack growth segments $r_1^\pm/r_1^o$ for Case I (τ_∞; E_∞)

Material	$E_\infty/\tau_\infty \times 10^{-3}$ (Vm/N)						
	-15	-10	-5	0	5	10	15
PZT-4	0.672	0.765	0.874	1	1.143	1.302	1.478
PZT-5H	0.675	0.742	0.851	1	1.191	1.422	1.695

$$\frac{a}{r_1} = \frac{a + r_1}{r_2} = \frac{a + r_1 + r_2}{r_3} = \cdots = \text{const.} \tag{19}$$

The results $r_1^+/r_1^o > 1$ for $+E_\infty$ and $r_1^-/r_1^o < 1$ for $-E_\infty$ is similar to those found for in-plane crack extension [6]. A sign change in E_∞ alters the ways with which the electrical and mechanical properties of the material would interact with external disturbance. This causes the crack to grow longer for $+E_\infty$ and shorter for $-E_\infty$.

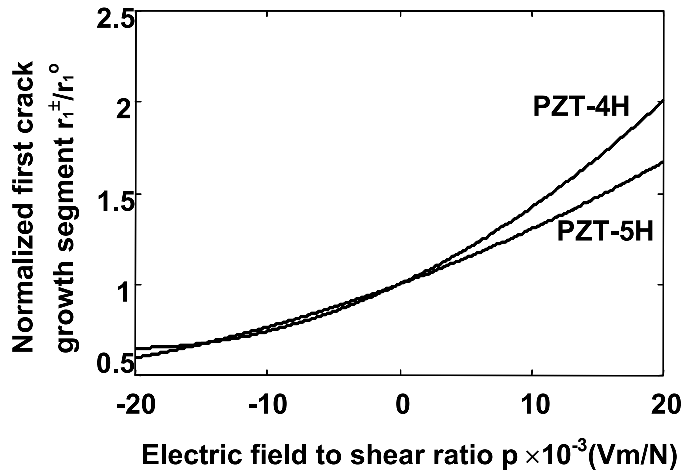

Figure 2: Normalized crack growth segment as a function of electric field to shear stress ratio

4.3 Case II: positive and negative electric displacement

When strain γ_∞ and electric displacement D_∞ are specified on the remote portion of the boundary, Fig. 1(a), the coupling of the electrical and mechanical properties would react differently when the direction of the electric displacement D_∞ is changed. This can be exhibited by solving for S in eq. (16) for the PZT-4 and PZT-5H materials. Following the exact procedure as discussed earlier for Case I and eq. (15), the numerical values of $S_1^\pm/S_1^o$ are first obtained. Application of eq. (18) gives $r_1^\pm/r_1^o$ from which eq. (19) gives the other growth steps $r_j^\pm/r_j^o$ for j = 2, 3, etc. The results for the first step are outlined in Table3.

TABLE 3

Normalized first crack growth segments $r_1^\pm/r_1^o$ for Case II (γ_∞; D_∞)

Material	D_∞/γ_∞ (C/m^2)						
	-15	-10	-5	0	5	10	15
PZT-4	2.880	2.103	1.477	1	0.673	0.459	0.467
PZT-5H	1.894	1.535	1.237	1	0.824	0.708	0.653

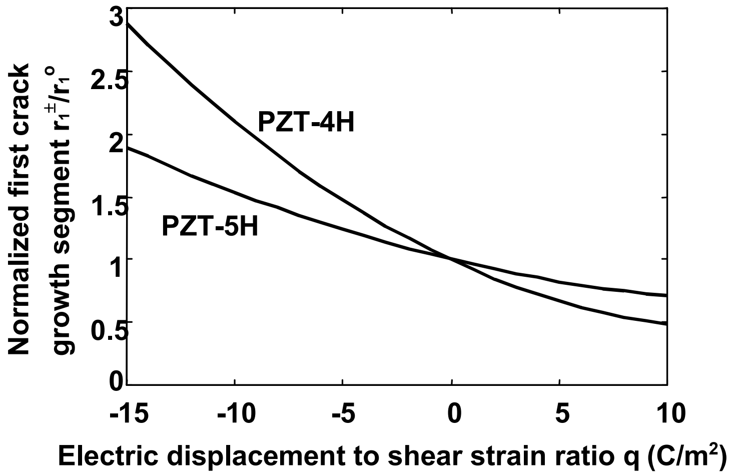

Figure 3: Normalized crack growth segment as a function of electric displacement to shear strain ratio

In contrast to Case I for specifying (τ_∞, E_∞), the crack growth behavior for Case II where (γ_∞, D_∞) are prescribed reacts in an opposite manner. Negative D_∞ decreases crack growth while positive D_∞ decreases crack growth. Such a trend is displayed in Fig. 3. The curves also intersect at q = 0 and $S/(\gamma_\infty^2 a/4 \in_{11}) = 1$. However, their slopes are negative instead of being positive as those in Fig. 2. For Case I. These results are new and are expected to prevail for in-plane a crack extension as well.

5. CONCLUSIONS

Further application of the volume energy density criterion show the enhancement/retardation behavior of crack growth in anti-plane shear is the same as that for in-plane crack extension [5,6]. However, when the stress/electric field boundary conditions are replaced, a reversal of the enhancement/retardation behavior is predicted. Using $D_\infty = 0$ as the base, crack growth would be increased for negative D_∞ and decreased for positive D_∞. These effects are just the opposite to those for prescribing E_∞ and τ_∞.

Experimental verifications of the above findings for anti-plane shear crack growth are impractical because it is next to impossible for producing a pure longitudinal shear mode. Some degree of opening mode would always be present ahead of a tunnel crack especially for the ceramic-like materials that are hard and brittle. The aim of this work is to provide the motivation for solving the electric displacement/strain boundary-value problem for in-plane crack extension. Displacement boundary condition experiments could be designed and performed to show that positive D_∞ would retard crack growth whereas negative D_∞ would enhance crack growth. This is contrary to the observations made in [1,2] for crack growth under the electric field/stress boundary conditions.

References

1 Tobin and Y.E. Pak, Effects if electric fields on fracture behavior of PZT ceramics. Smart Materials, ed. V.K. Varadan, SPIE Vol.1916, pp.78-86, 1993.

2 Y. E. Pak and A. Tobin, On the electric field effects in fracture of piezoelectric materials. Mechanics of Electromagnetic Materials and Structures, AMD-Vol.161/MD-Vol.42, ASME, 1993.

3 H. Gao, T. Y. Zhang and P. Tong, Local and global energy release rates for an electrically yielded crack in a piezoelectric ceramic. J. Mech. Phys. Solids, 45 (1997), 491-510.

4 S. Park and C. T. Sun, Fracture criterion of piezoelectric ceramics. J. Am. Ceram. Soc., 78 (1995), 1475-1480.

5 J.Z. Zuo and G.C. Sih, Energy density formulation and interpretation of cracking behavior for piezoelectric ceramics, J. of Theoretical and Applied Fracture Mechanics, 34 (1) 2000, 17-33.

6 G.C. Sih, J.Z Zuo, Multiscale behavior of crack initiation and growth in piezoelectric ceramics, J. of

Theoretical and Applied Fracture Mechanics, 34(2000) 123-141.
7 Y.E. Pak, Crack extension force in a piezoelectric material, J. of Applied Mechanics, 57(1990) 647-653.
8 Y.E. Pak, Linear elecro-elastic fracture mechanics of piezoelectric material, Int'l J. of Fracture (54) (1992) 79-100.
9 G.C. Sih, Mechanics of Fracture, Volume I to VII, Sijhoff and Noordhoff International Publisher, The Netherlands, 1973-1981.
10 G.C. Sih, Mechanics of fracture initiation and propagation, Kluwer Academic Publishers, The Netherlands, 1991.
11 G.C. Sih, Fracture mechanics of engineering structural components, Fracture Mechanics Methodology, G.C. Sih, L. Faria, eds., Martinus Nijhoff Publishers, The Netherlands, 35-101 (1984).